

## Attosecond Beats in Sodium Vapor

D. DeBeer, E. Usadi, and S. R. Hartmann

*Columbia Radiation Laboratory and Department of Physics, Columbia University, New York, New York 10027*

(Received 11 January 1988)

Transient, time-delayed, four-wave mixing (TDFWM) experiments have been performed on the Na *D* doublet with use of a novel angled-beam geometry. The effects of petahertz superposition-state modulations have been observed in the integrated TDFWM signal as a function of the time delay. As the time delay is varied, the lowest-order mixing signal modulates with a period of 980 as—corresponding to the sum frequency of the two Na *D* lines. Higher-diffraction-order mixing signals contain modulation components at integral multiples of the doublet sum frequency.

PACS numbers: 42.65.Ma, 32.90.+a, 42.50.Md, 42.65.Ft

Research on ultrafast phenomena is characterized by a mixture of techniques and instrumentation of varied nature.<sup>1,2</sup> Several practical schemes provide light pulses in the middle femtosecond regime and recent developments now yield excitation pulses with durations as short as 6 fs.<sup>3</sup> Less direct methods using broad-band light sources have the potential of exploiting short autocorrelation times in order to study ultrafast phenomena by way of transient four-wave mixing.<sup>4-10</sup> These latter experiments have been shown to be capable of obtaining both spectroscopic and relaxation information in the picosecond and femtosecond regimes. The extension of this technique to a much shorter time regime is promising. In the ultrafast regime, the establishment of a well defined delay time poses a potential difficulty because of

the angling of the excitation beams with respect to each other. This problem is relevant, however, only when we make relaxation measurements, not when we look at modulation effects.

The observation of high-frequency modulation effects in time-delayed four-wave mixing (TDFWM) does not require the use of broad-band excitation pulses when relaxation times are long. This is best seen by our viewing the modulation process not as a consequence of superposition-state modulation<sup>11</sup> but rather as due to an interference of scattering processes<sup>12</sup> from atomic gratings produced by excitation of separate atomic optical transitions. In a previous study<sup>11</sup> involving modulation beats the outputs of two conventional lasers, tuned separately to the two Na *D* lines, were combined to create an excitation field of the form

$$E = E_0 \{ e^{-i\Omega t} [e^{i\mathbf{k}_1 \cdot \mathbf{r}} + e^{i\mathbf{k}_2 \cdot \mathbf{r} - i\Omega \tau}] + e^{-i\Omega' t} [e^{i\mathbf{k}'_1 \cdot \mathbf{r}} + e^{i\mathbf{k}'_2 \cdot \mathbf{r} - i\Omega' \tau}] \} + \text{c.c.}, \quad (1)$$

where the primed and unprimed  $\mathbf{k}$  vectors correspond to the frequencies  $\Omega$  and  $\Omega'$ , and  $\tau$  is a variable relative delay between the prompt and delayed fields which are indicated by the subscripts 1 and 2, respectively. The optics were adjusted so that  $\mathbf{k}_1 - \mathbf{k}_2 \cong \mathbf{k}'_1 - \mathbf{k}'_2$ .<sup>11</sup> A mixing signal is generated with wave vector  $2\mathbf{k}_2 - \mathbf{k}_1$  which modulates at the difference frequency  $\Omega' - \Omega$  as a function of  $\tau$ . In the case of the Na *D*-line excitations the difference frequency is 530 GHz resulting in a modulation with a period of 1.9 ps. Similar results have been seen with use of broad-bandwidth excitations in atomic vapors of both Na<sup>10</sup> and Rb.<sup>7</sup> In the case of the Rb *D* line the difference frequency is much larger yielding a beat with a period of 139 fs. To see such beats in the attosecond regime the difference frequency would have to be in the petahertz regime. Alternatively, attosecond beats can be realized by the adjustment of the beams so that  $\mathbf{k}_1 - \mathbf{k}_2 = -(\mathbf{k}'_1 - \mathbf{k}'_2)$ , whereupon the modulation frequency is the sum rather than the difference of the individual excitation frequencies. The penalty is that mixing signals are no longer (see Ref. 11) produced when

the excitation pulses are delayed by an amount greater than their pulse duration.

The origin of the sum-frequency beats may be understood in terms of a simple induced-grating analysis. With the double-frequency excitation field given by Eq. (1), each resonant component generates an atomic grating with spacing  $2\pi/|\mathbf{k}_1 - \mathbf{k}_2|$ . This grating scatters the wave labeled  $\mathbf{k}_2$  by an angle  $n\theta$  (for scattering order  $n$ ), where  $\theta$  is the angle between  $\mathbf{k}_1$  and  $\mathbf{k}_2$ . The two gratings formed by the resonant excitations at  $\Omega$  and  $\Omega'$  are themselves separated by  $(\Omega' + \Omega)\tau/|\mathbf{k}_1 - \mathbf{k}_2|$  so that the phase shift  $\Delta\Phi$  in the two scattered waves at  $\Omega$  along  $n\theta$  is just  $\Delta\Phi = n(\Omega' + \Omega)\tau$ . As a result, sum-frequency modulations are expected in the interfering four-wave mixing signals as a function of  $\tau$ . This simplified analysis is correct only for  $n=1$  where it includes all scattering pathways. The correct expression for the modulation behavior for all  $n$  is obtained by direct calculation of the induced polarization from a step-function excitation field of the form of Eq. (1) on a three-level system whose levels are sufficiently separated so that the resonant excitations are effectively isolated. This yields

$$\mathcal{P}(t) = [\mathbf{P}\Omega_R \sin(\Omega(t - \tau) - \mathbf{k}_2 \cdot \mathbf{r}) + \mathbf{P}'\Omega'_R \sin(\Omega't - \mathbf{k}'_1 \cdot \mathbf{r})](\sin ft)/f, \quad (2)$$

where

$$f^2 = 4\Omega_R^2 \{1 + \cos[\frac{1}{2}(\Omega + \Omega')\tau] \cos[\frac{1}{2}(\Omega' - \Omega)\tau + (\mathbf{k}_2 - \mathbf{k}_1) \cdot \mathbf{r}]\},$$

$\mathbf{P}$  and  $\mathbf{P}'$  are the dipole moments for the  $\Omega$  and  $\Omega'$  transitions,  $\Omega_R$  and  $\Omega'_R$  are the associated Rabi frequencies, and we have assumed the  $\mathbf{k}_1 - \mathbf{k}_2 = -(\mathbf{k}'_1 - \mathbf{k}'_2)$  geometry. Setting  $\Omega'_R = \Omega_R$  and considering only the terms phased to radiate in the directions  $\mathbf{k}_2 + n(\mathbf{k}_2 - \mathbf{k}_1)$  ( $n > 0$ ) we have  $\mathcal{P} = \sum_{n=1}^{\infty} \mathcal{P}_n$ , where

$$\begin{aligned} \mathcal{P}_n(t) = & \left\langle \frac{\cos(n\phi) \sin(2\Omega_R t \{1 + \cos[\frac{1}{2}(\Omega' + \Omega)\tau] \cos\phi\}^{1/2})}{2\{1 + \cos[\frac{1}{2}(\Omega' + \Omega)\tau] \cos\phi\}^{1/2}} \right\rangle \\ & \times (\mathbf{P} \sin\{\Omega(t - \tau) - [\mathbf{k}_2 + n(\mathbf{k}_2 - \mathbf{k}_1)] \cdot \mathbf{r} - \frac{1}{2}n(\Omega' - \Omega)\tau\} \\ & + \mathbf{P}' \sin\{\Omega't - [\mathbf{k}'_1 + n(\mathbf{k}_2 - \mathbf{k}_1)] \cdot \mathbf{r} - \frac{1}{2}n(\Omega' - \Omega)\tau\}). \end{aligned} \quad (3)$$

The angle brackets indicate an average over a variable  $\phi$  introduced in the definition of a  $\delta$  function used in the evaluation of a series expansion of  $(\sin ft)/f$ . For fixed  $\phi$  the  $n$ th component,  $\mathcal{P}_n$ , of the induced dipole moment,  $\mathcal{P}$ , is a periodic function of  $(\Omega' + \Omega)\tau$  with period  $4\pi$ . However, on our averaging over  $\phi$  the moment  $\mathcal{P}_n$  becomes an odd or even function of  $\cos[\frac{1}{2}(\Omega' + \Omega)\tau]$  according as  $n$  is odd or even. As a consequence  $\mathcal{P}_n^2(t)$  (the output signal) is an even function of  $(\Omega' + \Omega)\tau$  with period  $2\pi$ . In addition, the output signals have the same modulation whether one looks at either  $\Omega$  or  $\Omega'$  separately or at both simultaneously.

The detailed behavior of  $\mathcal{P}_n$  is readily obtained in the limit of either small or large pulse area  $\Omega_R t$ . Working first in the small-angle limit and keeping only the lowest-order term radiating at  $\Omega$  we have

$$\mathcal{P}_n(t) = (-1)^n \frac{2^n}{(2n+1)!} (\Omega_R t)^{2n+1} \cos^n \left[ \frac{\Omega' + \Omega}{2} \tau \right] \mathbf{P} \sin \left\{ \Omega(t - \tau) - [\mathbf{k}_2 + n(\mathbf{k}_2 - \mathbf{k}_1)] \cdot \mathbf{r} - n \frac{(\Omega' - \Omega)}{2} \tau \right\}. \quad (4)$$

The radiated intensity emitted into the  $n$ th order is thus

$$I_n \propto \int (\mathcal{P}_n^* \cdot \mathcal{P}_n) dt \propto [\frac{1}{2} + \frac{1}{2} \cos((\Omega + \Omega')\tau)]^n. \quad (5)$$

As the scattering order  $n$  increases, the scattering signal width, measured by the value of  $\tau$  for which  $I_n$  decreases to  $\frac{1}{2}$ , decreases. No higher-frequency beat terms are directly observable; the sum-frequency beats dominate to all orders of scattering.

In the limit of large pulse areas,  $\Omega_R t \gg 1$ , Eq. (3) yields a sharpened modulation pattern which narrows with increasing pulse area and is independent of  $n$  for moderate  $n$ . We write below a general expression for  $\mathcal{P}_n$ . The character of the last expression is determined by the fact that the average over  $\phi$  in Eq. (3) is dominated by contributions near  $\phi = 0$  and  $\pm\pi$ :

$$\begin{aligned} \mathcal{P}(t) = & \mathbf{P} \sin\{\Omega(t - \tau) - [\mathbf{k}_2 + n(\mathbf{k}_2 - \mathbf{k}_1)] \cdot \mathbf{r} - \frac{1}{2}n(\Omega' - \Omega)\tau\} \\ & \times \begin{cases} 0, & \text{for } (\Omega' + \Omega)\tau = \pi, 3\pi, 5\pi, \dots, \\ [(-1)^n / \sqrt{8}] J_0(2\epsilon \Omega_R t) & \text{for } (\Omega' + \Omega)\tau \cong 0, 2\pi, 4\pi, \dots, 2m\pi, \dots, \\ \text{where } \begin{cases} \eta = n, \epsilon^2 = 2 \sin^2[\frac{1}{4}(\Omega + \Omega')\tau] & \text{if } m \text{ is even,} \\ \eta = 0, \epsilon^2 = 2 \cos^2[\frac{1}{4}(\Omega + \Omega')\tau] & \text{if } m \text{ is odd,} \end{cases} \\ \left[ 8\pi \Omega_R t \cos \left[ \frac{\Omega' + \Omega}{2} \tau \right] \right]^{-1/2} \begin{cases} \frac{\sin(2\Omega_R t \{1 + \cos[\frac{1}{2}(\Omega' + \Omega)\tau]\}^{1/2} - (\pm \frac{1}{4}\pi))}{\{1 + \cos[\frac{1}{2}(\Omega' + \Omega)\tau]\}^{1/4}} \\ + \frac{\sin(2\Omega_R t \{1 - \cos[\frac{1}{2}(\Omega' + \Omega)\tau]\}^{1/2} + (n \pm \frac{1}{4})\pi)}{\{1 - \cos[\frac{1}{2}(\Omega' + \Omega)\tau]\}^{1/4}} \end{cases}, & \text{otherwise,} \end{cases} \end{cases} \quad (6)$$

where we use  $+$  or  $-$  according as  $\cos[\frac{1}{2}(\Omega' + \Omega)\tau]$  is greater or less than 0. The scattering half-width  $\tau_w$  is determined by the condition  $J_0(x) = 1/\sqrt{2}$  so that  $\tau_w \cong \sqrt{2}/[(\Omega' + \Omega)\Omega_R t]$  independent of  $n$ . For a pulse area  $\Omega_R t \approx 10\pi$  the

modulation spikes will narrow to  $1/100$  of the modulation period. It is important to note that the amplitudes of these peaks reach an asymptotic value and do not disappear in the large-pulse-area limit. In the valleys between the peaks the polarization tends to zero as  $1/(\Omega_R t)^{1/2}$ . This result implies that sharp modulation patterns will appear in experiments using cw lasers.

We have performed TDFWM experiments in Na vapor. The experimental apparatus is shown in Fig. 1. The dye-laser pulses were 7 ns in duration and were tuned to 589.6 and 589.0 nm, the wavelengths of the sodium  $3S_{1/2}-3P_{1/2}$  and  $3S_{1/2}-3P_{3/2}$  transitions, respectively. Each laser operated in four or five longitudinal modes, yielding an overall laser bandwidth of 5 GHz. The beam geometry  $\mathbf{k}_1 - \mathbf{k}_2 = -(\mathbf{k}'_1 - \mathbf{k}'_2)$  was imposed; since  $\Omega$  and  $\Omega'$  are nearly equal this can be satisfied (to within the beam divergence) by our making  $\mathbf{k}_1 \parallel \mathbf{k}'_2$  and  $\mathbf{k}_2 \parallel \mathbf{k}'_1$ . To accomplish this the dye-laser outputs were split and recombined to provide two double-frequency pulses in such a way that the 589.0-nm component was delayed by  $\tau$  in one beam and the other frequency component delayed by the same amount in the other beam. Since the delays introduced in the two beams must be stable compared to the period of the modulation, the relative positions of the beam splitter, corner cube, and translating mirror shown in Fig. 1 had to be stable to much better than a wavelength; also this portion of the apparatus had to be enclosed to prevent the effect of air currents changing the effective delay. The two double-frequency beams were angled at  $\theta \approx 0.3$  mrad to overlap spatially throughout a 100-mm-long sodium cell. A pinhole in the focal plane of a 300-mm lens passed only the TDFWM signal in the phase-matched  $\mathbf{k}_2 + n(\mathbf{k}_2 - \mathbf{k}_1)$  direction. The signal was detected with an EG&G model FND-100 photodiode and integrated over its full 7-ns duration. The TDFWM signal was monitored as the relative delay was varied by the movement of mirror M1. The first-order signal presented in Fig. 2 as a func-

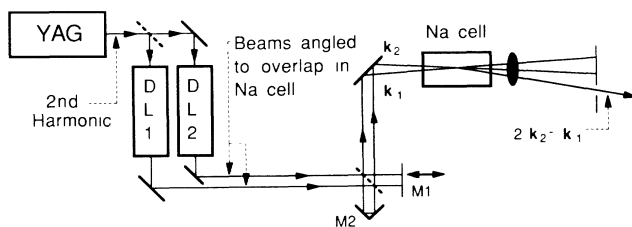


FIG. 1. Schematic diagram of the experimental apparatus used to generate TDFWM in the sum-frequency geometry (for  $n=1$ ). Mirror M1 is mounted on a precision translation stage which provides for variable relative delays of up to 30 fs in increments of  $< 100$  as. The delay was calibrated with a HeNe interferometer. M2 is a corner cube which displaces each beam so that it combines at the beam splitter with the beam of the other frequency.

tion of  $\tau$  is a simple sinusoid as would be predicted in the low-pulse-area limit of Eq. (5). The depth of modulation is less than would be expected from theory because of imperfect spatial overlap of the excitation pulses in the sample and the difficulty in setting  $\Omega_R = \Omega'_R$ . All our theoretical results yield the instantaneous TDFWM signal while we measure its integrated value. This would matter if the experimental modulation pattern varied with pulse area but we find no evidence for any such variation. Our agreement with Eq. (5) is obtained even though the excitation pulses were not in the small-pulse-area limit. We have not observed any of the predicted narrowing of the modulation signal that is expected with the multiple  $\pi$  excitations with which we worked. Nor have we seen the narrowing of the peaks and flattening of the valleys expected from Eq. (6) when the sum-frequency signals are scattered into higher orders ( $n > 1$ ). We believe that both these experiments are sensitive to vibrational instabilities in our apparatus which average out the higher harmonic frequencies.

We eliminate the influence of vibrational instabilities on modulation narrowing by performing the above experiment using the difference-frequency geometry ( $\mathbf{k}_1 - \mathbf{k}_2 = \mathbf{k}'_1 - \mathbf{k}'_2$ ) of Ref. 11. With this geometry and looking at the first order,  $n=1$ , scattering signal we obtain (except for the time scale) a simple sinusoidal pattern similar to that shown in Fig. 2. When we look at higher-order scattering signals we find narrowed modulation patterns with increasing narrowing as  $n$  increases. In Fig. 3 we show the fourth-order,  $n=4$ , scattering signal superimposed on the theoretical expectation given in Eq. (5). The agreement is very good. Here, as in the sum-frequency case, the excitation pulse areas were large. Again the modulation pattern seemed insensitive to pulse intensity although this was not explored systematically.

The observation of modulation narrowing at high

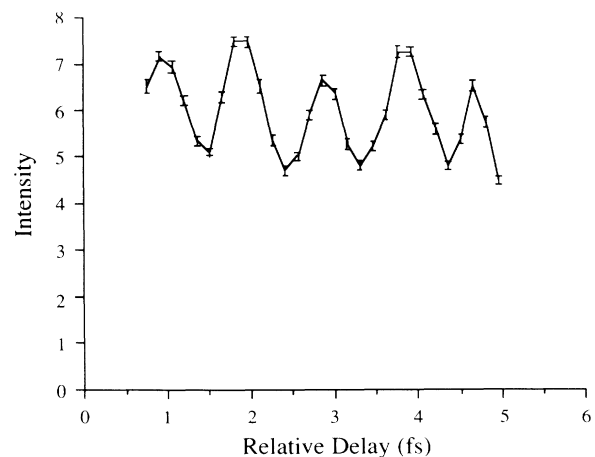


FIG. 2. Typical set of data for the sum-frequency geometry: signal intensity vs relative pulse delay. The Na vapor was held at a temperature of 470 K.

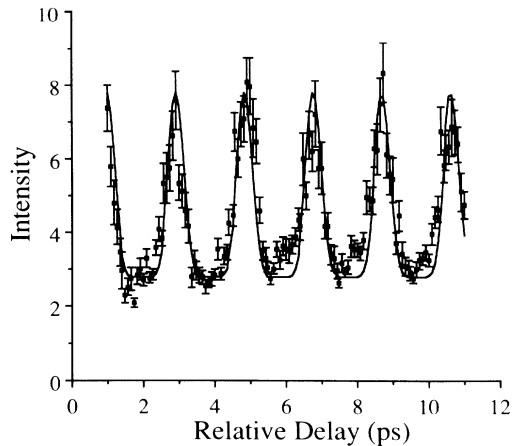


FIG. 3. Data taken in the difference-frequency geometry showing the narrowing of the modulation in a high diffraction order ( $n=4$ ).

scattering order when we work with the difference-frequency geometry supports our suspicion that vibrational instabilities prevented their observation in the sum-frequency mode. Our continued inability to observe modulation narrowing at large excitation pulse area remains unresolved. One possible explanation may lie in the fact that our experiments have all been done with optically thick samples whose optical densities were in the range of 10 to 100. All our analysis assumes optically thin samples. The optically thick regime is complicated and we worked there in order to obtain signals which we could differentiate from the noise.

Sum-frequency beat observation depends on the simultaneous excitation of two distinct transitions sharing a common ground state. The foregoing analysis respects this restriction and does not allow the limit  $\Omega' \rightarrow \Omega$  with both lasers tuned to the same transition. The expected result in this degenerate case is that the modulation in the TDFWM signal has the period of the optical frequency  $\Omega$ , as in interferometry, and not  $2\Omega$ . This is most easily understood via the simple induced-grating analysis by the inclusion of the (previously) moving-grating component due to the product of the fields at  $\Omega$  and  $\Omega'$ . We took considerable care in looking for the sum-frequency beat using a single laser whose output was split to serve as a double source. Working this way we saw only the resonant beats and not the sum-frequency beats. We did not look at the higher-diffraction-

order signals which we calculate should narrow according to  $I_n \propto [\frac{1}{2} + \frac{1}{2} \cos(\Omega\tau)]^{2n+1}$  similar to the case of the sum-frequency beats.

In summary, the new phenomenon of sum-frequency beats in a four-wave mixing experiment has been documented and its origin explained. By extension, the presence of beats in the TDFWM signal has been shown to depend critically on the excitation beam geometry and to provide spectroscopic information of a varied but well defined character. As faster processes are studied broader bandwidth excitations will be used which will in turn couple multiple transitions, resulting in complex signal modulations. Sum- and difference-frequency geometries may be separately employed to untangle confusing spectroscopic details. Last, we note that the existence of sum-frequency beats and their narrowing with scattering order and excitation intensity may allow development of more accurate position transducers.

We thank R. Friedberg for insightful contributions, F. W. Kantor for stimulating comments, and B. Brody for assistance in preparing the manuscript. This work was supported by the U.S. Office of Naval Research and by the Joint Services Electronics Program (U.S. Army, U.S. Navy, U.S. Air Force) under Contract No. DAAG 29-85-K-0049.

<sup>1</sup>See, for example, *Ultrafast Phenomena V*, edited by G. R. Fleming and A. E. Siegman (Springer-Verlag, Berlin 1986).

<sup>2</sup>N. J. Rosker, F. W. Wise, and C. L. Tang, *Phys. Rev. Lett.* **57**, 321 (1986).

<sup>3</sup>R. L. Fork, C. H. Brito Cruz, P. C. Becker, and C. V. Shank, *Opt. Lett.* **12** 483 (1987).

<sup>4</sup>N. Morita and T. Yajima, *Phys. Rev. A* **30**, 2525 (1984).

<sup>5</sup>Hiroki Nakatsuka, Makato Tomita, Masahiro Fujiwara, and Shuji Asaka, *Opt. Commun.* **52**, 150 (1984).

<sup>6</sup>Masahiro Fujiwara and Ryo Kuroda, *J. Opt. Soc. Am. B* **2**, 1634 (1985).

<sup>7</sup>J. E. Golub and T. W. Mossberg, *Opt. Lett.* **11**, 431 (1986).

<sup>8</sup>Toshiaki Hattori, Akira Terasaki, and Takayoshi Kobayashi, *Phys. Rev. A* **35**, 715 (1987).

<sup>9</sup>Kenji Kurokawa, Tosiaki Hattori, and Takayoshi Kobayashi, *Phys. Rev. A* **36**, 1298 (1987).

<sup>10</sup>R. Beach, D. DeBeer, and S. R. Hartmann, *Phys. Rev. A* **32**, 3467 (1985).

<sup>11</sup>D. DeBeer, L. G. Van Wagenen, R. Beach, and S. R. Hartmann, *Phys. Rev. Lett.* **56**, 1128 (1986).

<sup>12</sup>Y. R. Shen, *The Principles of Nonlinear Optics* (Wiley, New York, 1984).

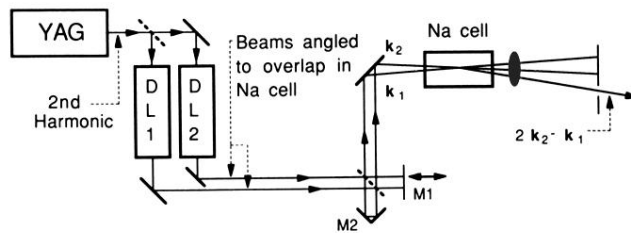


FIG. 1. Schematic diagram of the experimental apparatus used to generate TDFWM in the sum-frequency geometry (for  $n=1$ ). Mirror M1 is mounted on a precision translation stage which provides for variable relative delays of up to 30 fs in increments of  $< 100$  as. The delay was calibrated with a HeNe interferometer. M2 is a corner cube which displaces each beam so that it combines at the beam splitter with the beam of the other frequency.